

An Acoustic Approach for Detection of Developmental Dysplasia of Hip

T. Hassan*, L. McKinney, R.H. Sandler, A. Kassab, C. Price, F. Moslehy, H.A. Mansy

1. Department of Mechanical and Aerospace Engineering, University of Central Florida, Orlando, Florida, USA
2. College of Medicine, University of Central Florida, Orlando, Florida, USA
{thassan@knights., lukemckinney@knights., hansen.mansy@}ucf.edu

Abstract— An acoustic non-invasive approach for detection of Developmental Dysplasia of Hip (DDH) was investigated. The proposed method was tested using different benchtop simplified models of the hip joint. Models were stimulated with band-limited white acoustic noise (10-2500 Hz) and the response of the model was measured. The transfer function, coherence, and phase were determined for different simulated hip dysplasia levels and for simulated normal cases. Results showed that the transfer function, coherence and phase were affected by dysplasia occurrence. Larger effects were seen for more simulated severe dysplastic hips. This suggests that the proposed approach may have potential for DDH detection. Further investigations in animal models and humans are warranted to document accuracy of the proposed approach.

Keywords: *Developmental, dysplasia, hip, Signal Processing, Acoustic, Vibration.*

I. INTRODUCTION

Developmental dysplasia of the hip (DDH) in neonates is common with approximately 2-3 per thousand neonates suffering from the condition [1]. It is widely known that early intervention of patients with DDH show a decreased rate of late presentation. [2], while delayed detection leads to deferred and less effective treatment resulting in chronic disability in these children. Current screening methods in infants include certain physical examination techniques (e.g., the Ortolani and Barlow maneuvers), but these require significant skill and training to perform reliably. Similarly, ultrasonography can be used as screening tool, however due to its utility in low resource settings it is limited by equipment availability and need for highly trained professionals [3], [4]. Therefore, for primary care providers in the USA, especially for developing regions, it would be useful to develop new non-invasive, easy to use, and accurate tools for DDH detection.

Different techniques utilizing sound waves for screening of DDH were proposed. Kwong et al. [5] reported a method where a mild sound waves were applied at the sacrum and sound signals were measured at both hips (at the greater trochanters) by two microphones installed in two stethoscope heads. Results showed that the coherence of sound transmitted to the two hips was high (0.89-0.96) for preschoolers, neonates and adults. The highest coherence was found in the adult group, whereas the lowest coherence was found in the preschool group. Overall, the neonate's coherence was slightly lower than

the adults in that study. A second study [6], used the same technique and found a significant difference between the normal neonates and patients with unilateral DDH. A discrepancy parameter was calculated and a cut-off discrepancy of 2.0 dB achieved a sensitivity of 100% in detecting DDH. Frequency bands that were most effective were around 200, 250, and 315 Hz. Safa et al. [7] reported that dysplastic hips had lower sound transmission values than normal hips in a study of 22 patients (average age 5.9 years; range 0.3-14 years). In that study patients were tested in four positions: a) hips and knees neutrally positioned and measurements performed between the patella and the pubis symphysis, b) hips and knees neutrally positioned and measurements performed between the patella and the anterior superior iliac spine (ASIS), c) hips and knees positioned at 45 degree and 90 degree of flexion, respectively, and measurements performed between the patella and pubis symphysis, and d) hips and knees positioned at 45 degree and 90 degree of flexion, respectively, and measurements performed between the patella and the ASIS. In each position, the sound generator was placed on the patella and the receiver was applied on the pubis symphysis and ASIS. It was shown that sound transmission values of dysplastic hips were always lower than that of normal hips when the hip and knee were flexed. It was also shown that sound transmission values decreased with age. The current investigation uses a similar approach to that of previous studies, but utilizes benchtop models with simplified geometries to help elucidate the basic acoustic changes associated with DDH. Previous studies suggested that changes in transfer function and coherence correlate with DDH. These parameters are investigated in the current study in addition to the phase delay, which is a new parameter not explored before.

II. MATERIALS AND METHODS

A. Benchtop Models

Different simplified benchtop models were constructed: a) a model consisting of two aluminum bars, b) a 3D printed model of a ball and socket joint, and c) 3D printed model of femur and ilium including the acetabulum. In the first model, the two aluminum bars were 1.3 cm in diameter and 4 cm long. They had mechanical properties comparable to bone. More specifically, the aluminum modulus of elasticity is 69 GPa while the modulus for cancellous bone is about 76 GPa. The speed of sound

through aluminum alloys ranges from 3040-6420 m/s and the average speed of sound through bone is 3514.9 m/s.

The first 3D model was a simplified representation of the connection between the femur and acetabulum. This model is made of ABS (Acrylonitrile Butadiene Styrene) plastic. While the material properties of this model are different from bone, its overall shape resembled the coupling between the femoral head and acetabulum. Hence, this model was used to explore the effects of changes in that coupling due to DDH.

The third model included ABS 3D printed parts that simulate the femur and Ilium, using geometry extracted from CT scans of the hip and femur.

B. Hardware and Analysis

A computer-controlled system was constructed to generate and measure acoustic signals. The computer was connected to a data acquisition module (Model: NI USB-6211, National Instruments, Austin, TX). A MATLAB code was written to generate a white noise (50-2500 Hz) signal, to acquire two acoustic signals, and to calculate the transfer function, phase and coherence between the two acquired signals.

The stimulus signal generated by the computer was amplified using a power amplifier (Model: TS200, Accel Instruments Corp., Irvine, CA) that drove an electromagnetic shaker (Model: 2007E, the Modal Shop Inc., Cincinnati, OH.). The shaker then introduced the stimulus signal into the model to be tested.

Two uniaxial accelerometers (Model 352C65, PCB Piezotronics, Depew, NY) were used to detect the stimulus and the transmitted signals. A multi-channel charge amplifier (Model: 480B21, PCB Piezotronics,

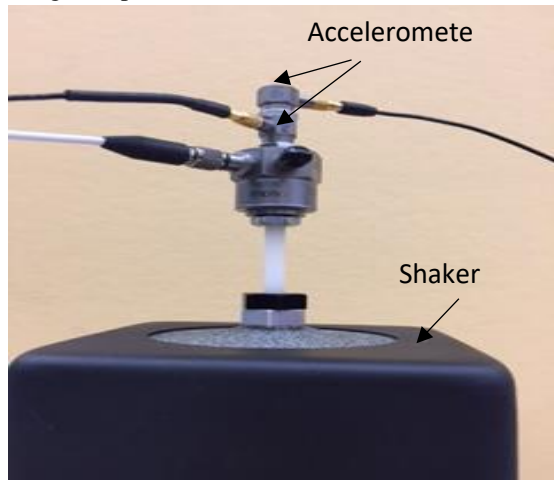


Figure 1. Shaker and the two sensors used in the current experiment.

Depew, NY) amplified the accelerometer output. The shaker and accelerometers are shown in Figure 1. (The third accelerometer that can be seen in the figure below that two labeled accelerometers is not used in the current experiment.)

The following equations were used to calculate the transfer function ($TF_{12}(f)$) [8], coherence ($\gamma_{12}(f)$) and phase delay ($\phi_{12}(f)$) [9] between two signals x, y:

$$TF_{xy}(f) = \frac{P_{xy}(f)}{P_{xx}(f)} \quad (1)$$

$$\gamma_{xy}(f) = \frac{(|P_{xy}(f)|)^2}{(P_{xx}(f))(P_{yy}(f))} \quad (2)$$

$$\phi_{xy}(f) = \tan^{-1} \left(\frac{\text{Imaginary } P_{xy}(f)}{\text{Real } P_{xy}(f)} \right) \quad (3)$$

Here, P_{xy} is the cross power spectrum between the two signals, P_{xx} is the power spectrum of the first signal and P_{yy} is the power spectrum of the second signal. Coherence quantifies the association between the two signals as a function of frequency and is bound by 0 and 1. A coherence value of 1 indicates the strongest association. To obtain accurate transfer function, coherence and



(a) Aluminum bars with 0 degree angle (b) Aluminum bars with 35 degree angle



(c) Aluminum bars with 50 degree angle (d) Aluminum bars with 90 degree angle

Figure 2. Setup of aluminum bars with different angles.

phase, spectra were calculated based on the average of multiple measurements [10].

The accelerometers were calibrated before performing all experiments. Calibration was done by attaching the two accelerometers to the shaker as shown in Figure 1. Then the transfer function, coherence and phase were determined.

Figure 2 shows the setup utilizing the two aluminum bars. Here the lower bar bottom edge was stimulated by the shaker. These aluminum bars were used to simulate the connection between the femoral head and acetabulum at different tilt angles. By changing the angle between the two rods, the surface contact between the rods was altered. This allows quantification of the effects of these geometrical changes on acoustic transmission. Three different angles between the bars were considered: 35°, 50°, and 90°. To measure the acoustic signal at the

stimulus and detection locations, one accelerometer was affixed at the stimulus point (bottom of the lower bar) while the other accelerometer was affixed at the upper end of the top bar. Accelerometer wax (PCB Piezotronics, Depew, NY) was used to couple the accelerometers to their respective locations.

Figure 3 shows the 3D printed model of a simplified hip joint. The model consisted of two parts. One part was the simplified femur and the other was the simplified acetabulum and ilium. Since the femur is typically tilted by 33-38 degrees when measuring the acetabular index [11], the simulated femur was tested at a tilt angle of 35 degrees.



(a) Case 0: Femoral head completely inside acetabulum (b) Case 1: Femoral head partially inside acetabulum



(c) Case 2: Femoral head outside the acetabulum (d) Case 3: Femoral head completely outside the acetabulum.

Figure 3. Setup of different hip joints for the 3D printed model with different connecting points between the femoral head and ilium. These include cases where the femoral head is inside and outside the acetabulum.



(a) Case 0: normal (no dysplasia) (b) Case 1: onset of dysplasia (IHDI grade 1)



(c) Case 2: moderate dysplasia (IHDI grade 3) (d) Case 3: severe dysplasia (IHDI grade 4)

Figure 4. Setup of different hip joints for realistic model with different angles.

Tests were done with the simulated femur in a) case 0: the normal position (femoral head fully inside the acetabulum) and b), c), d) case 1-3: at 3 different displaced stages. In all cases the accelerometer wax was used to affix the simulated femur to the desired contact point of the simulated ilium. The accelerometer locations were at the top and bottom points of the model as can be seen in Figure 3.

Figure 4 shows a more realistic model of the femur, ilium and an acetabulum. The femoral head and acetabulum were polished to better simulate the real case.

The model dimensions were extracted from an actual CT. Four different cases were studied in this model: a) case 0: normal hip, b) case 1: the smallest level of dysplasia where the femoral head is touching the acetabulum but not throughout the contact surface, which corresponds to the International Hip Dysplasia Institute (IHDI) [12] Grade 1 dysplasia, c) case 2: femoral head rests on the rim of the acetabulum (IHDI grade 3), and d) case 3: femoral head is completely outside the acetabulum and touching the ischial body of the ilium (IHDI grade 4). The stimulus and first accelerometer was placed at the distal articulating surface of the femur (since there is no patella in this model) while the second accelerometer was placed at the iliac crest.

III. RESULTS

A. Calibration

Calibration results are shown in Figure 5 where the transfer function, coherence and phase between the 2 accelerometers are displayed. The results of the

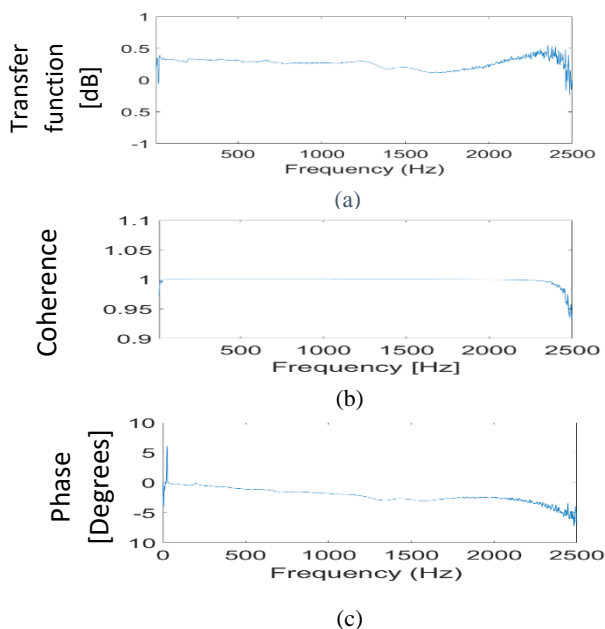
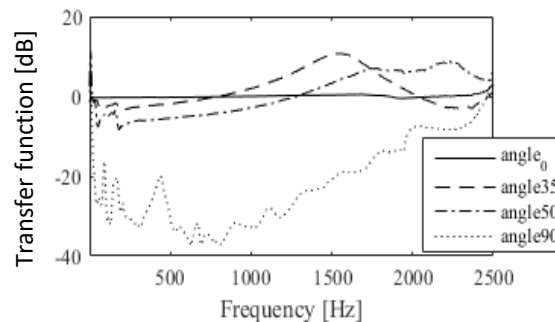
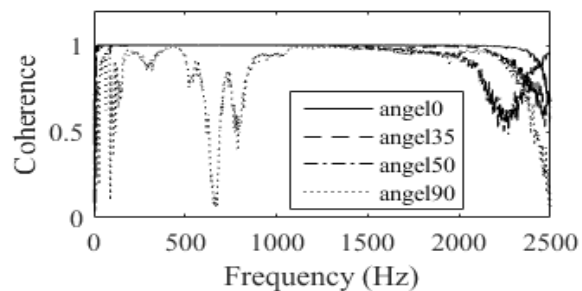


Figure 5: (a) Transfer function, (b) Coherence, and (c) Phase delay between the two accelerometers during calibration.

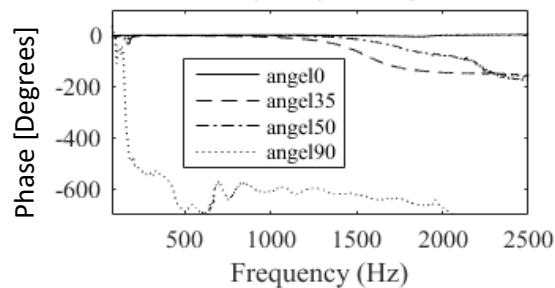
calibration showed that in the frequency range of interest (10-2000 Hz), the TF was within ± 0.5 dB, coherence was $> 95\%$, and the phase was 0 ± 5 degrees.



(a) Transfer function comparison for model 1 at different tilt angles (geometry shown in Fig 2). When rods were fully touching (angle=0), transmission was equally efficient at all frequencies as expected. When angle increased, there was a gradual loss of transmission in the 50-600 Hz frequency band.



(b) The coherence function for model 1. Coherence was close to 1 for most cases except the case with the largest angle; where heavily attenuated transmitted signals lead to lowered coherence.

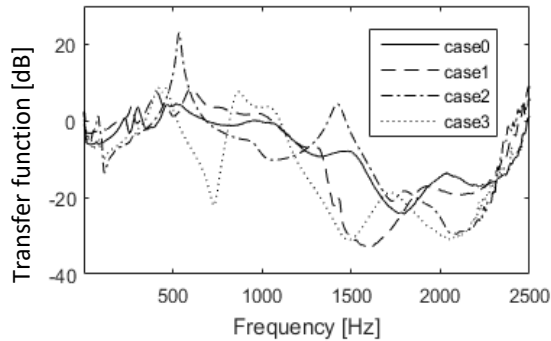


(c) Phase angle between the two accelerometer signals for model 1. The phase was close to zero when the two bars were aligned. A very small angle is expected in this case due to the high speed of sound. At higher angles, the angle remained small but the phase delay became noticeable at higher frequencies which suggests additional delay at the connection between the two rods possibly due to nonlinearities. For the 90 degree case, the delay may not be reliable since the transmitted signal was significantly inhibited.

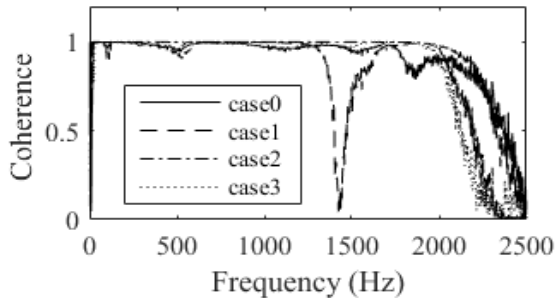
Figure 6: (a) Transfer function, (b) Coherence, and (c) Phase delay of first simplified model of Figure 2.

B. First Simplified Model

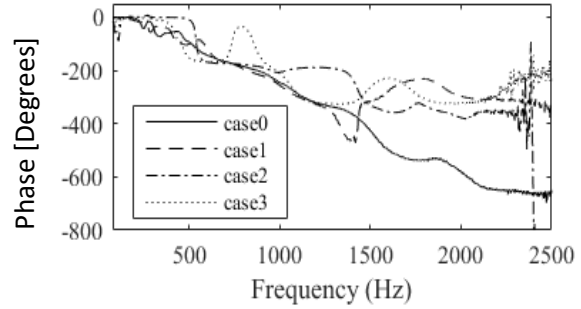
The results of the first model are shown in Figure 6 for four different angles. It can be seen in Figure 6a that the transfer function was close to 0 dB (± 0.5 dB, $50\text{Hz} < f < 2000\text{Hz}$) when rods were fully touching (angle = 0). This suggests equally efficient transmission at all frequencies (as expected) because of optimal coupling between the two rods at this angle. When the angle increased, there was a gradual loss of transmission in the 50-600 Hz frequency band. The peaks that appear in the spectrum at higher frequencies are probably due to system resonances. The coherence was high for most cases signifying high correlation between the input and output signals. This suggests a strong association between the stimulus and the transmitted signal. This is possibly due to the high simplicity in the model that allows efficient transmission and relatively low nonlinear effects and resonances, except at the 90 degree case, where low transmitted signal amplitudes resulted in loss of coherence. Figure 6c shows the Phase angle between the two accelerometer signals. The phase was nearly zero (± 5 degrees, $50\text{Hz} < f < 2000\text{Hz}$) when the two bars were aligned. A very small phase delay is expected in this case



(a) Transfer function comparison for model 2 for the normal and displaced cases. The complexity of the transfer function is likely due to the models complex geometry. However, there was a drop in transfer function for the dysplasia cases in most of 100- 2300 Hz frequency band. The drop in TF was small (0-20 dB) but noticeable at certain frequencies.



(b) Coherence function for model 2 (shown in Figure 3). The coherence was close to 1 except for high frequencies and around 1400 Hz, where the signal experienced low amplitudes.



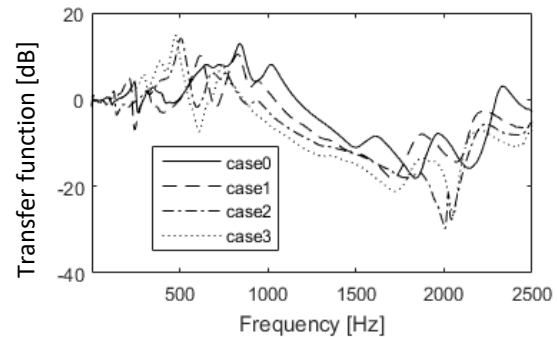
(c) Phase angle between the two accelerometer signals for model 2. The phase (especially for case 0) appears linear with frequency which is consistent with a fixed time delay (i.e., fixed speed of sound of about 150 m/s).

Figure 7: (a) Transfer function, (b) Coherence, and (c) Phase delay for the 3D printed model of Figure 3.

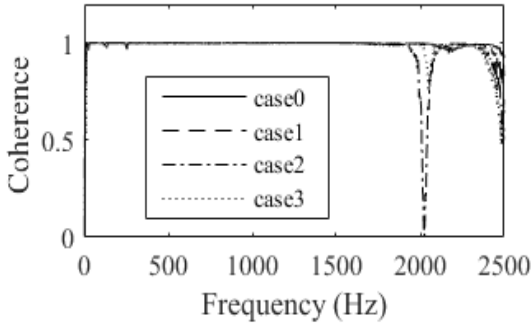
since the speed of sound is significantly high. At higher angles, the angle remained small but phase delay became noticeable at high frequencies, which suggests additional delay at the connection between the two rods possibly due to nonlinearities. For the 90 degree case, the phase delay may not be reliable since the transmitted signal was significantly inhibited.

C. 3D Printed Model of Simplified Hip Joint

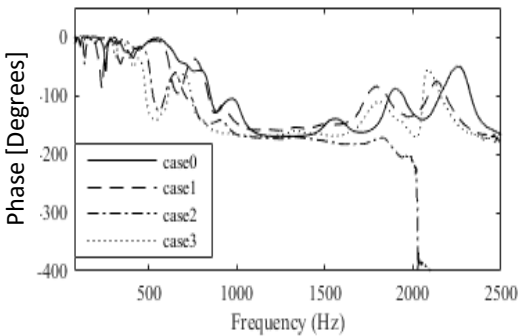
The results of the second model are shown in Figure 7 for four different cases (case: 0-3). It can be seen in Figure 7a that when severity of dysplastic hips increased, there was a loss of transmission in most of the 100-2300 Hz frequency band. Case 2 exhibited noticeable resonances around 500 and 1500 Hz. The coherence was high for most cases suggesting strong association between the stimulus and the transmitted signal except for a drop in coherence around 1400 Hz for case 1. The reason is possibly due to the low signal amplitudes resulted in loss of coherence. Figure 7c shows Phase angle between the two accelerometer signals. The phase appears linear with



(a) The transfer function comparison for model 3 for the normal and displaced cases (Geometries are shown in figure. 4). There was a drop in the transfer function for the dysplastic cases for most of the 600-2500 Hz frequency range. The TF drop was small (0-20dB) but noticeable at certain frequencies.



(b) Coherence function for model 3. The coherence was close to 1 except for high frequencies and around 2000Hz where the signals experienced low amplitudes.



(c) Phase angle between the two accelerometer signals for model 3. Phase delay tended to increase with frequency and approached 180 degrees at high frequencies (1100 -1600 Hz).

Figure 8: (a) Transfer function, (b) Coherence, and (c) phase delay of 3D printed model of simplified femur and ilium of Figure 4.

frequency which is consistent with a fixed time delay (and hence frequency independent speed of sound).

D. 3D printed model of simplified femur and ilium

The results of the first model are shown in Figure 8 for 4 different cases. It can be seen in Figure 8a that there was a drop in the transfer function for the dysplastic cases in most of the 600-2500 Hz frequency band. The coherence was close to 1 except for high frequencies (>2300 Hz) and at around 2000Hz (case: 2) that experienced low signal amplitudes resulted in loss of coherence. Figure 8c shows the phase angle between the two accelerometer signals. Phase delay was noticeable and tended to approach 180 degrees at high frequencies (1100-1600 Hz), which has similarity to the response of some systems containing inertia and stiffness.

IV. CONCLUSION

The objective of this study was to build and test an acoustic technique for screening of DDH in neonates. Simplified benchtop models were constructed,

stimulated with acoustic signals, and sound transmission was measured. The transfer function, coherence, and phase were determined for simulated normal hip geometry and for simulated hip dysplasia. Results showed that simulated hip dysplasia inhibited sound transmission which was demonstrated by changes in the transfer function, coherence and phase. The magnitude of these changes correlated with the simulated degree of hip dysplasia. This suggests possible utility for detection of DDH. Future studies will include testing on humans and animals using the same method. A portable device will be used to excite the subject and accelerometers will be attached to the subject to record the sound transmission. We will test the patients using the same parameters to measure the validity of our method. If results from this future experiment are found to be favorable, this approach may be followed to detect DDH.

REFERENCES

- [1] C. Price and B. Ramo, "Prevention of hip dysplasia in children and adults," *Orthopedic Clinics of North America*, vol. 43, pp. 269-279, 2012.
- [2] D. Jones, "Neonatal Detection Of Developmental Dysplasia Of The Hip (DDH)," *J Bone Joint Surg [Br]*, vol. 80, pp. 943-945, 1998.
- [3] F. Moore, "Examining infants' hips-can it do harm?," *J Bone Joint Surg [Br]*, vol. 71, pp. 4-5, 1989.
- [4] M. Uzel, G. Ergun, and H. Ekerbicer, "The knowledge and attitudes of the primary care physicians on developmental dysplasia of the hip," *Saudi Medical Journal*, vol. 28, pp. 1430-1434, 2007.
- [5] K. Kwong, X. Huang, J. Cheng, and J. Evans, "Acoustic transmission in normal human hips: structural testing of joint symmetry," *Medical Engineering & Physics*, vol. 25, pp. 811-816, 2003.
- [6] K. Kwong, X. Huang, J. Cheng, and J. Evans, "New Technique for early screening of developmental dysplasia of the hip: pilot study," *Journal of Pediatric Orthopaedics*, vol. 23, pp. 347-351, 2003.
- [7] M. Kapicoglu, and F. Korkusuz, "Diagnosis of development dislocation of the hip by sonospectrography," *Clinical Orthopaedics and Related Research*, vol. 466, pp. 802-808, 2008.
- [8] H. Vold, J. Crowley, and G. T. Rocklin. "New Ways of Estimating Frequency Response Functions," *Sound and Vibration*, vol. 18, pp. 34-38, 1984.
- [9] R. N. Bracewell, *The Fourier Transform and Its Applications*. New York, USA: McGraw-Hill, 1983.
- [10] S. M. Kay, *Modern spectral estimation : theory and application*. Englewood Cliffs, New Jersey, USA: Prentice Hall, 1988.
- [11] L. Laborie, I. Engesaeter, T. Lehmann, F. Sera, C. Dezauteux, L. Engesaeter, and K. Rosendahl, "Radiographic measurements of hip dysplasia at skeletal maturity—new reference intervals based on 2,038 19-year-old Norwegians," *Skeletal Radiol*, vol. 42, pp. 925-935, 2013.
- [12] U. Narayanan, K. Mulpuri, T. Lehmann, W. Sankar, N. Clarke, H. Hosalkar, and C. Price, "Reliability of a New Radiographic Classification for Developmental Dysplasia of the Hip," *Journal of Pediatric Orthopaedics*, vol. 35, pp. 478-484, 2015.